

## Barium and molybdenum records in bivalve shells: Geochemical proxies for phytoplankton dynamics in coastal environments?

Julien Thébault,<sup>a,\*</sup> Laurent Chauvaud,<sup>b</sup> Stéphane L'Helguen,<sup>c</sup> Jacques Clavier,<sup>a</sup> Aurélie Barats,<sup>d,1</sup> Séverine Jacquet,<sup>e</sup> Christophe Pécheyran,<sup>d</sup> and David Amouroux<sup>d</sup>

<sup>a</sup> Université de Bretagne Occidentale, Laboratoire des Sciences de l'Environnement Marin (UMR CNRS/IRD/UBO 6539), Institut Universitaire Européen de la Mer, Technopôle Brest-Iroise, Plouzané, France

<sup>b</sup> CNRS, Laboratoire des Sciences de l'Environnement Marin (UMR CNRS/IRD/UBO 6539), Institut Universitaire Européen de la Mer, Plouzané, France

<sup>c</sup> CNRS, Laboratoire de Chimie Marine (UMR CNRS/UPMC 7144), Roscoff, France

<sup>d</sup> CNRS, Equipe de Chimie Analytique Bio-Inorganique et Environnement (UMR CNRS/UPPA 5254), Institut Pluridisciplinaire de Recherche sur l'Environnement et les Matériaux, Pau, France

<sup>e</sup> IRD, Unité de Recherche Camélia (UR 103), Nouméa, New Caledonia

### Abstract

Barium:calcium and molybdenum:calcium ratios were investigated in shells of the tropical scallop *Comptopallium radula*. Three juvenile specimens were harvested alive in the southwest lagoon of New Caledonia after a 1-yr hydrological survey. Calcite samples representing a few hours of biomineralization were laser-ablated along the maximal growth axis and analyzed for Ba and Mo content with an inductively coupled plasma mass spectrometer. Absolute dates of shell precipitation assigned on the basis of periodic formation of shell growth patterns led to the accurate reconstruction of ontogenetic variations of elemental ratios with subweekly resolution. Interindividual variability of Ba:Ca and Mo:Ca time series was low, indicating an environmental control on the incorporation of these elements within shells. Both profiles were characterized by a background level punctuated by sharp peaks. The ingestion of diatoms enriched in Ba (adsorbed on iron oxyhydroxides associated with the frustules) is the most likely cause of the formation of Ba:Ca peaks. Some contribution of diatom-associated barite is also possible. In every instance, Ba:Ca would possibly be a proxy for the timing and magnitude of diatom blooms. Among all the theories that could be advanced to explain the occurrence of Mo:Ca peaks, the most plausible appears to be the ingestion of phytoplankton cells grown on  $\text{NO}_3^-$ , and therefore containing high levels of Mo required for the activity of nitrate reductase. If this is so, then Mo:Ca could be a new proxy for nitrate uptake by phytoplankton in coastal ecosystems, helping to reconstruct the balance between new and regenerated production in paleoenvironments.

### Introduction

Although they account for <1% of the total photosynthetic biomass, phytoplankton are the true lungs of the Earth, being responsible for >45% of the total oxygen production of the biosphere (Field et al. 1998). Recognized as a major component of the global carbon cycle, this invisible forest can also soften the effect of climate change, helping limit the increase of atmospheric  $\text{CO}_2$  through the biological pump by trapping carbon from the atmosphere and storing it in the deep sea. In addition, phytoplankton are the basis of all ocean food chains, supplying food for higher trophic levels; therefore, they are a good indicator of the overall health of ocean ecosystems and fisheries.

Given this ecological importance, assessments of past phytoplankton dynamics are necessary for a better understanding of ancient carbon and nutrient cycles, paleoclimate changes, variations of past fish stocks and yields, and

socioeconomic changes of human communities depending on marine resources. Such paleoproductivity datasets covering the latest Holocene are also extremely useful to place constraints on the respective roles of anthropogenic forcings and natural variations on the changes currently observed in the functioning of marine ecosystems, which include: changes in primary production level (Sarmiento et al. 2004), changes in the composition of phytoplankton communities (Miller et al. 2006), and modification of the efficiency of  $\text{CO}_2$  uptake through changes in circulation and vertical mixing (Ittekkot et al. 1996). Finally, paleoproductivity datasets are necessary to test and refine climate models dedicated to the prediction of the future of marine ecosystems.

Instrumental records of primary productivity, however, are extremely scarce in time and space; uninterrupted records only exist since the first satellites came into operation during the late 1970s. For times and places without direct observation, paleoceanographers rely on records of measurable proxy parameters. For several decades, many studies have focused on the use of minor and trace element concentrations archived in sediment cores as proxies for past variations of several environmental parameters (see the review by Henderson 2002). A diverse array of biological and geochemical proxies has been exploited in sediments to reconstruct past changes of biological productivity and to

\* Corresponding author: julien.thebault@univ-brest.fr

<sup>1</sup> Present address: Université de Nice Sophia Antipolis, Institut de Chimie de Nice (FR CNRS 3037), Laboratoire de Radiochimie et des Sciences Analytiques et Environnement (EA 1175), Nice, France.

infer how the export of carbon has changed through time; these proxies include accumulation of calcium carbonate, opal, and organic matter; changes in foraminiferal assemblage; and accumulation rates of marine barite ( $\text{BaSO}_4$ ), excess accumulation of aluminum (Al) and barium (Ba), and ratios of Ba: titanium (Ti) and Al: Ti (Averyt and Paytan 2004). However, the temporal resolution of such reconstructions is low, generally coarser than decades. Therefore, efforts have been made to assess the potential of trace element content in marine biogenic carbonates, especially bivalve mollusk shells, as high-resolution proxies for past phytoplankton dynamics (Stecher et al. 1996; Vander Putten et al. 2000; Gillikin et al. 2006).

Mollusk shell growth occurs by periodic accretion of calcium carbonate layers. This recurrent shell growth provides the basis for assigning calendar dates to each successive increment of accreted shell material. In contrast to corals and varved sediments, most mollusks form distinct and easily discernable circadian, circalunidian, or ultradian growth structures and, therefore, provide information on subseasonal variations of paleoenvironmental conditions (e.g., Schöne et al. 2005). In the past decade, many studies highlighted the presence of sharp increases in Ba concentration over a background level in shells of several bivalve mollusk species, including: *Mercenaria mercenaria* and *Spisula solidissima* (Stecher et al. 1996), *Mytilus edulis* (Vander Putten et al. 2000; Gillikin et al. 2006), *Saxidomus giganteus* (Gillikin et al. 2008), *Pecten maximus* (Barats et al. 2007; Gillikin et al. 2008), *Mesodesma donacium*, and *Chione subrugosa* (Carré et al. 2006). Most studies suggested a linkage between phytoplankton blooms and the formation of Ba peaks in these shells. However, it is still unclear whether this linkage is direct, through the ingestion of Ba-rich phytoplankton cells, or indirect, through the ingestion of  $\text{BaSO}_4$  crystals formed in settling phytoplankton flocs right after blooms. This second hypothesis was recently refuted by Gillikin et al. (2008), who concluded that Ba: calcium (Ca) peaks in *P. maximus* and *S. giganteus* shells are caused by an as yet undetermined environmental forcing. After ingestion, Ba is delivered to the site of mineralization through Ca channels (Markich and Jeffree 1994) and is finally bound to the crystal lattice (Takesue et al. 2008). Besides Ba, no other trace element has been identified in bivalve shells as a potential proxy for phytoplankton dynamics. However, some analytical techniques (e.g., laser ablation coupled to an inductively coupled plasma mass spectrometer [LA-ICP-MS]; Gray 1985) allow the accurate measurement of tens of elements archived in biogenic carbonates within a few seconds. Their abiding improvement considerably increases the probability of discovering new paleoceanographic proxies. In a preliminary study performed in shells of the great scallop *P. maximus*, Barats et al. (2007) investigated the temporal variations of concentrations of 16 elements with LA-ICP-MS. This exploratory study highlighted extremely intriguing molybdenum (Mo) concentration time series in shells, presenting common patterns with Ba records.

Here, we present records of Ba: Ca and Mo: Ca ratios in bivalve mollusk shells. We focused on juvenile scallops,

*Comptopallium radula* (Linnaeus 1758), collected in the southwest lagoon of New Caledonia after a 1-yr environmental survey. The aims of this paper are (1) to analyze the behavior of Mo in *C. radula* shells and relate it to the Ba record in the same shells, (2) to review thoroughly the different biogeochemical processes that can be put forward to explain the temporal variations of these elemental ratios in shells, and (3) to assess the potential of these trace elements as proxies for describing phytoplankton dynamics in coastal environments.

## Methods

New Caledonia is an archipelago located in the southwest Pacific Ocean, 1500 km east of Australia (19–23°S, 163–168°E; Fig. 1A). The main island is surrounded by a 1500-km-long barrier reef enclosing a 21,700 km<sup>2</sup> lagoon (Fig. 1B). It is subject to an oceanic tropical climate characterized by four seasons. The warm and wet season, also called cyclonic season, lasts from December to March. It is followed by a transition period in April and May during which temperature and rainfall strongly decrease. The cool season lasts from June to August, a period during which low-pressure systems coming from the Tasman Sea sometimes hit New Caledonia with heavy rainfall. This season is finally followed by a dry transition season from September to November.

Our study site is located in the southeastern part of Sainte-Marie Bay (southwest lagoon; 22°18.22'S, 166°28.89'E), close to Nouméa, the capital of New Caledonia (Fig. 1C). This shallow-water site (5 m depth), with a substrate consisting of muddy sands, is sheltered from dominant trade winds (blowing from the east-southeast). Water residence time in the bay is <4 d (Bujan 2000). The closest river (Coulée River) is located 15 km northeastward (Fig. 1C).

A hydrological survey was performed at this site from August 2002 to July 2003. Bottom-water temperature was recorded hourly with an EBRO EBI 85A thermal probe fixed 30 cm above the sediment. Bottom-water salinity was measured weekly with a SeaBird SBE19 profiler and is reported in accordance with the Practical Salinity Scale. Water samples were collected weekly 1 m above the sediment with a 5-liter Niskin bottle. They were used to determine percent oxygen saturation and ammonium ( $\text{NH}_4^+$ ), nitrate + nitrite ( $\text{NO}_3^- + \text{NO}_2^-$ , hereafter referred as  $\text{NO}_x^-$ ), chlorophyll *a* (Chl *a*), and pheophytin *a* (Pheo *a*) concentrations. Dissolved oxygen (DO) concentration was measured by the Winkler method, modified by Carpenter (1965). DO saturation concentration was calculated from temperature and salinity data according to Benson and Krause (1984).  $\text{NH}_4^+$  concentration was measured by the orthophthaldialdehyde-based fluorometric method developed by Holmes et al. (1999).  $\text{NO}_x^-$  concentration was measured according to the automated colorimetric procedure of Raimbault et al. (1990). Chl *a* and Pheo *a* concentrations were determined by the fluorometric method of Yentsch and Menzel (1963). Average daily flow of the Coulée River was obtained from the New Caledonian government's Observatory of Water Resources.

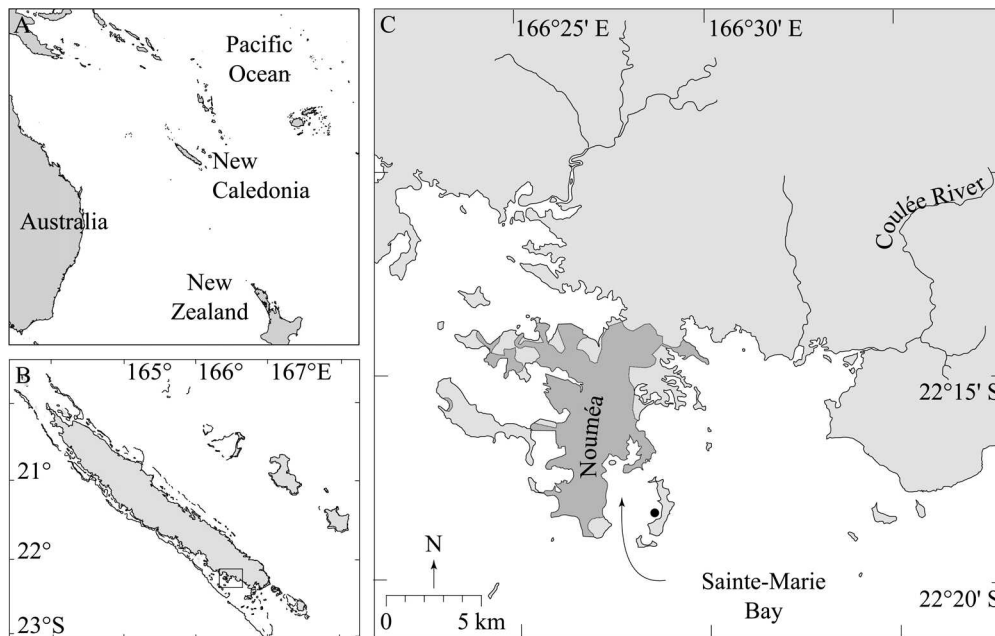


Fig. 1. (A) Location of New Caledonia in the southwest Pacific Ocean. (B) Map of New Caledonia. (C) Part of the southwest lagoon of New Caledonia around the peninsula of Nouméa (urbanized areas are displayed in dark gray). The black dot in Sainte-Marie Bay indicates the location of our study site.

*C. radula* (Fig. 2A) is a large (shell height up to 100 mm) sedentary filter-feeding scallop living under branching corals or on coralline fragment beds, generally between 0.5 and 5 m depth, in the tropical Indo-West Pacific Ocean. Its calcitic shell is textured with fine concentric striae formed with a 2-d periodicity (Fig. 2B; Thébault et al. 2006). Three juvenile specimens (shell height = 56.5–63.2 mm) were collected alive at the beginning of austral winter 2003. Juveniles were chosen because they have the largest annual increase in shell size (compared with mature specimens) and provide the highest temporal resolution in carbonate records. Their shells were cleaned by soaking in 90% acetic acid for 45–60 s to remove bio-fouling, rinsed with distilled water, and air dried. With a diamond saw, a

section ( $\sim 13 \times 40$  mm; Fig. 2A) was cut from each shell to fit into an ablation chamber.

Absolute Ba and Mo concentrations in shells were measured on these sections by LA-ICP-MS. An X7 Thermo Electron ICP-MS coupled to a Cetac LSX-100 ultraviolet (UV) laser ablation system was used with the parameters listed in Barats et al. (2007). Analyses were performed on the exterior surface of the shell. Although different from what was done in several other studies (analyses performed on the cross-sectional surface of the shell; Stecher et al. 1996), this method is commonly used in studies dealing with scallop shell geochemistry (Lorrain et al. 2005; Barats et al. 2007; Gillikin et al. 2008). A cleaning step consisting of laser preablation was conducted immediately before elemental analyses to

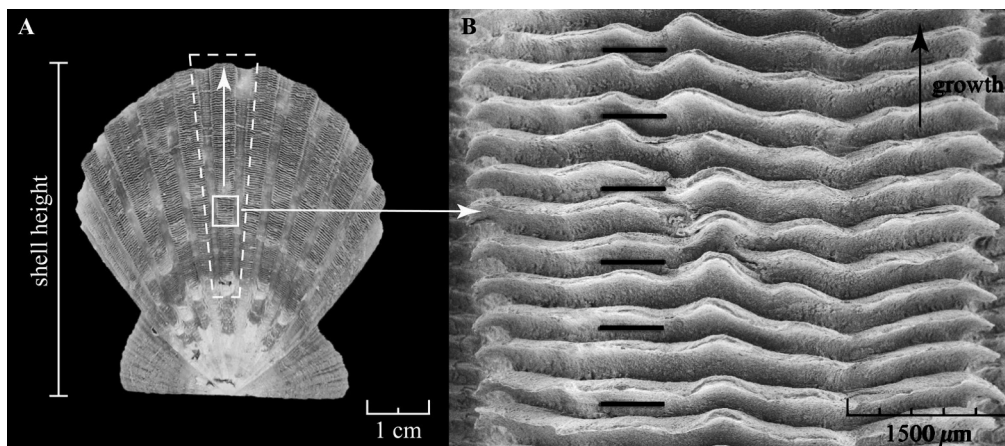


Fig. 2. Photographs of the upper surface of the left valve of *C. radula*. (A) Dashed line delimits the shell section inserted into the ablation chamber. The axis of maximal growth is indicated by the vertical white arrow. (B) Image (scanning electron microscopy) of striae taken along the axis of maximal growth. Shell samples ablated for elemental analysis can be readily identified (black lines).

remove shell surface contamination (adsorbed detrital material and other artifacts not associated with the time of biomineralization). One sample ( $525 \times 80 \mu\text{m}$ ) representing a few hours of biomineralization was ablated every two striae (i.e., every 4 d of growth) along the axis of maximal growth (Fig. 2B). During acquisition, signal intensities were recorded for  $^{43}\text{Ca}$ ,  $^{98}\text{Mo}$ , and  $^{138}\text{Ba}$ .  $^{43}\text{Ca}$  was used as an internal standard to correct for laser beam energy drift, focus variation at the sample surface, and ICP-MS drift. Element quantification was carried out with an in-house standard consisting of coprecipitated, metal-enriched  $\text{CaCO}_3$  powders pressed into compact pellets (Barats et al. 2007). Although these pellets cannot be considered matrix-matched standards, they definitely provide a closer matrix match than NIST glass standards (U.S. National Institute of Standards and Technology) commonly used for these kinds of studies. Absolute Ba and Mo concentrations were finally converted to molar ratios (Ba:Ca and Mo:Ca), assuming 100%  $\text{CaCO}_3$ . Detection limits were estimated from the signal intensities of argon blanks ( $3\sigma$ ) and were  $1.2 \times 10^{-3}$  and  $19.5 \times 10^{-3} \mu\text{mol mol}^{-1}$  for Ba:Ca and Mo:Ca ratios, respectively. Knowing the periodicity of striae formation, an absolute date of formation was finally assigned to each sample taken along the shell by backdating from the last stria (harvest date). It should be noted, however, that visual identification and counting of scallop striae are sometimes tricky and can lead to uncertainties in backdating (see Thébault et al. 2006). Moreover, shell growth cessations can occur during a few days as secondary effects of predation attempts (e.g., by crabs; L. Chauvaud unpubl.). Such short growth stops are hardly identifiable on the shell surface. Consequently, the timing of geochemical records comprises an uncertainty of a few days.

One of the specimens (hereafter referred as Shell No. 2) presented a clearly visible hiatus in shell growth on its external surface, corresponding to a period during which shell growth ceased (see Thébault et al. [2007] for more extensive explanations). Consequently, no record of elemental ratios was available for a 2.5-month period during the summer of 2002–2003. Moreover, striae abrasion in the umbonal region (Fig. 2A) prevented us from dating the oldest parts of the shells. Therefore, geochemical records only reached back to the beginning of August 2002 (Shell No. 2), the end of August 2002 (Shell No. 1), and mid-September 2002 (Shell No. 3).

An estimate of the amount of Ba and Mo incorporated daily within *C. radula* shells was made according to the following method (Fig. 3). On the basis of the periodicity of striae formation in *C. radula*, daily shell growth rates were calculated for each shell by measuring the growth increment width along the axis of maximal growth (Fig. 3A) by a method described in Chauvaud et al. (1998) (see fig. 3 in Thébault et al. [2007] for an overview of daily growth rates of these three shells). Knowing the final shell height of each specimen, these daily shell growth rates were used to compute the height of each shell for each consecutive day from August 2002 to their death (Fig. 3B). A biological survey including monthly sampling and dissection of 40 scallops (shell height = 28.5–107.2 mm) was conducted from August 2002 to August 2003 in the

southwest lagoon of New Caledonia (Thébault 2005) and was used to derive a relationship between *C. radula* shell height and shell dry weight (Fig. 4). Using this relationship, we calculated the evolution of the shell dry weight for each consecutive day (Fig. 3C) and the quantity of new shell material formed daily (Fig. 3D). The latter was used together with absolute Ba and Mo concentrations to estimate the quantity of Ba and Mo incorporated daily into each shell from August 2002 to their death (Fig. 3E). The underlying assumption, as yet unchecked, was that elemental ratios measured on the shell surface are representative of the bulk of the shell.

Pearson correlation coefficients were calculated to identify significant relationships between all of the measured geochemical, physical, chemical, and biological variables. Statistical analyses were performed with Statgraphics Plus 5.1 software.

## Results

*Hydrological survey*—Our hydrological survey covered the four seasons characterizing the oceanic tropical climate of New Caledonia and included a powerful tropical cyclone (Erica) that crossed New Caledonia on 14 March 2003 with gusts reaching  $56 \text{ m s}^{-1}$  in Nouméa. The results of this survey are representative of the whole range of environmental conditions that can be found in New Caledonia. From August 2002 to July 2003, mean daily bottom-water temperature ranged from  $20.4^\circ\text{C}$  to  $29.3^\circ\text{C}$  and presented a clear seasonal pattern, with highest values in the middle of the warm season (Fig. 5A). DO saturation ranged from 87% to 116%, with lowest values during the warm season (Fig. 5A) and was inversely correlated to temperature (Table 1). Coulée River flow was low from September to the beginning of December 2002 (dry season) and increased during the wet season, reaching  $106 \text{ m}^3 \text{ s}^{-1}$  after Cyclone Erica (Fig. 5B). Salinity presented small variations, ranging from 34.73 to 36.18 and exhibited a seasonal pattern over the study period. Low values were recorded from the end of the wet season to the beginning of the cool season (Fig. 5B). Salinity variations were negatively correlated to the Coulée River flow, but no significant relationship was observed with temperature (Table 1), suggesting that the variations resulted from dilution of seawater by fluvial inputs rather than from a balance between evaporation and precipitation. No salinity drop was measured following Cyclone Erica because of our sampling frequency (weekly), which was lower than water residence time in Sainte-Marie Bay (4 d).

Chl *a* concentration ranged from  $0.34$  to  $3.89 \mu\text{g L}^{-1}$  (Fig. 5C). The annual time series exhibited a background level around  $0.5 \mu\text{g L}^{-1}$ , punctuated with several small peaks between 1 and  $2 \mu\text{g L}^{-1}$ , and reached a maximum in late December 2002. Chl *a* concentration presented a highly significant correlation with DO saturation, suggesting that DO saturation variations were partly controlled by the balance between production and respiration (Table 1). Assuming a carbon (C):Chl *a* ratio of 50 (Charpy and Charpy-Roubaud 1990) and that organic carbon is 50% of phytoplankton dry weight (Strickland 1960), this Chl *a*

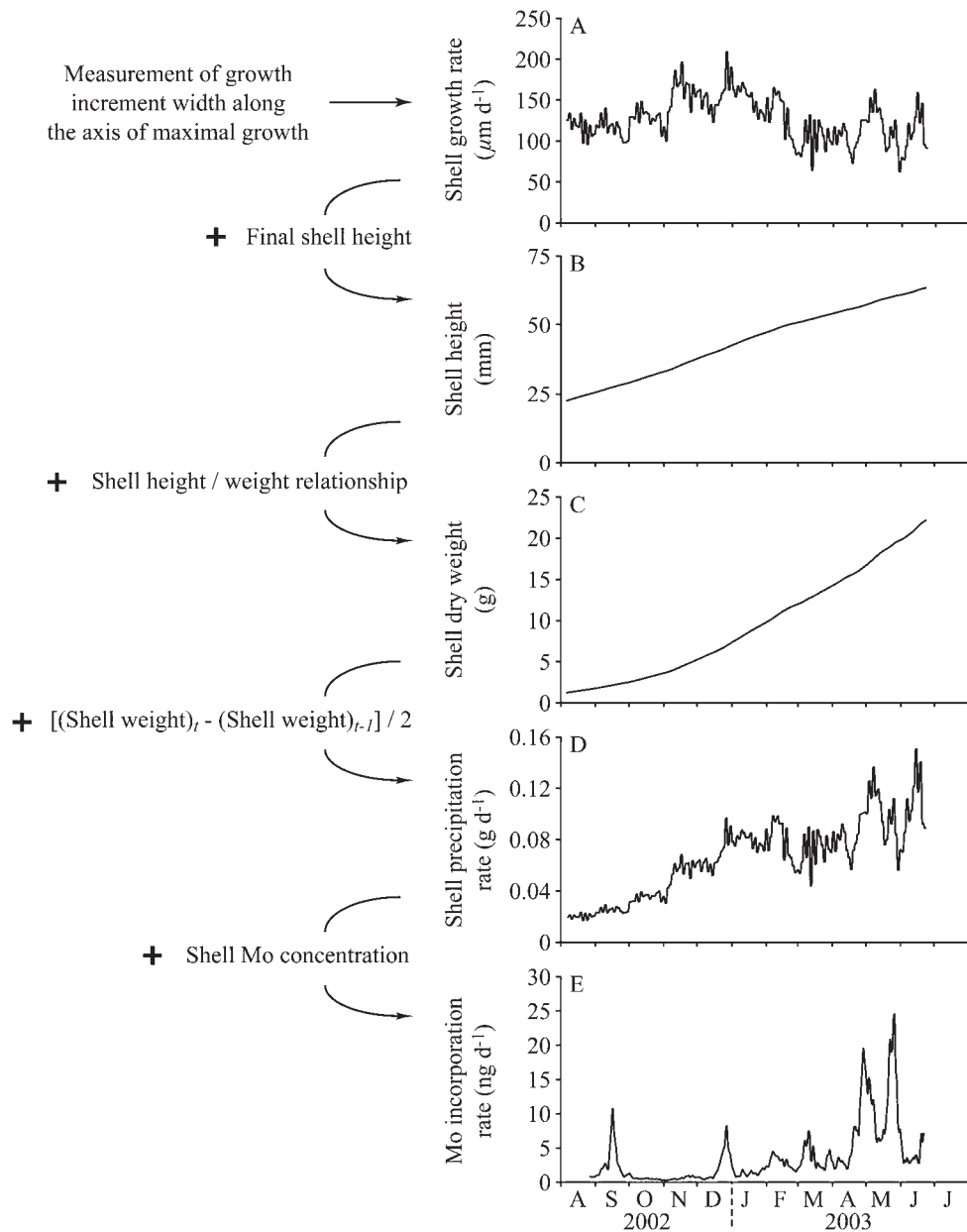


Fig. 3. Illustration of the method used to calculate daily rates of Ba and Mo incorporation into *C. radula* shells. These five plots were drawn from shell growth rate and Mo concentration data obtained on one of the three specimens studied in this paper. The same method was used for other specimens and for the calculation of Ba incorporation rates. Daily variations from August 2002 to July 2003 of (A) shell growth rate, (B) shell height, (C) shell dry weight, (D) shell precipitation rate, and (E) Mo incorporation rate.

concentration range corresponded to a dry phytoplankton biomass of 34–389  $\mu\text{g L}^{-1}$ . Pheo *a* concentration was quite low, ranging from 0.11 to 0.71  $\mu\text{g L}^{-1}$  over the survey, except on 28 May 2003 (2.70  $\mu\text{g L}^{-1}$ ; Fig. 5C). Chl *a* and Pheo *a* concentrations were significantly correlated (Table 1). Chl : Pheo mass ratio ranged from 0.6 to 8.8 during the survey, with only one value <1 (28 May 2003), indicating fresh phytoplankton populations and rapid organic matter degradation in the water column throughout our survey (Fig. 5C).  $\text{NH}_4^+$  concentration ranged from 0.02 to 1.85  $\mu\text{mol L}^{-1}$  (Fig. 5D).  $\text{NH}_4^+$  levels were relatively low from August to December 2002, except in September 2002 (1.6  $\mu\text{mol L}^{-1}$ ), high in April and May 2003, and maximal

in June 2003.  $\text{NO}_x^-$  concentration ranged from 0.01 to 1.83  $\mu\text{mol L}^{-1}$  (Fig. 5D) and presented seasonal variations similar to those of  $\text{NH}_4^+$  concentration (Table 1), suggesting that these two forms of inorganic nitrogen shared, to some extent, a common origin. In addition,  $\text{NH}_4^+$  and  $\text{NO}_x^-$  concentrations were both inversely correlated with salinity, suggesting that nitrogenous nutrients partly came from freshwater inputs (Table 1).

*Shell geochemistry*—Ba:Ca of the three specimens ranged from 0.242 to 4.508  $\mu\text{mol mol}^{-1}$  (Fig. 6A). All time series presented relatively similar variations from August 2002 to July 2003. High Ba:Ca ratios were recorded in

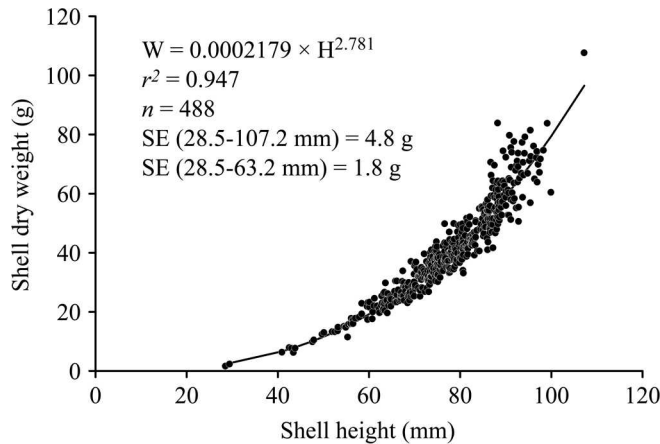


Fig. 4. Allometric relationship between *C. radula* shell height and shell dry weight derived from biometric measurements of 488 specimens. Also quoted are standard errors (SE) of this relationship for the whole dataset and for shell heights <63.2 mm (maximum shell height of our specimens).

August 2002 (Shell No. 2, no data for the other specimens), September 2002 (Shell Nos. 1 and 2, no data for Shell No. 3), March 2003 (all shells), and May 2003 (all shells). The highest values occurred in late December 2002 (Shell Nos. 1 and 3, no record in Shell No. 2 because of a growth stop between December 2002 and February 2003). Given

the low interindividual variability of the Ba:Ca time series (Fig. 6A), we built an average Ba:Ca profile (Fig. 7A). This average time series closely fit seasonal variations of Chl *a* concentration ( $r^2 = 0.699$ ,  $p < 0.001$ ; Table 1): both profiles were characterized by a relatively flat background level (around  $0.4 \mu\text{mol mol}^{-1}$  for Ba:Ca, i.e., two orders of magnitude above the detection limit) punctuated by several sharp peaks, and Chl *a* and Ba:Ca peaks were relatively synchronous and tended to be proportional (Fig. 7A). The highest Ba:Ca coincided with the main Chl *a* peak with a 5-d time lag. This time lag was similar in March 2003. On the other hand, the Ba:Ca peak recorded in May 2003 lagged  $\sim 13$  d behind the Chl *a* peak. It should be kept in mind, however, that these time lags are of the same order of magnitude as the uncertainty in the timing of geochemical records.

Mo:Ca ranged from 0.006 to  $0.423 \mu\text{mol mol}^{-1}$  and presented quite low interindividual variability (Fig. 6B). It varied dramatically over relatively short time periods, with episodic increases over a background level. Although the background level was higher than the detection limit, it was around or below the quantification limit (usually defined as three times the detection limit; Currie 1995). Any discussion on variations of the background level of Mo:Ca must then be considered with care. High Mo:Ca ratios were recorded in September 2002 (Shell Nos. 1 and 2, no data for Shell No. 3), from April to June 2003 (all shells), and, to a lesser

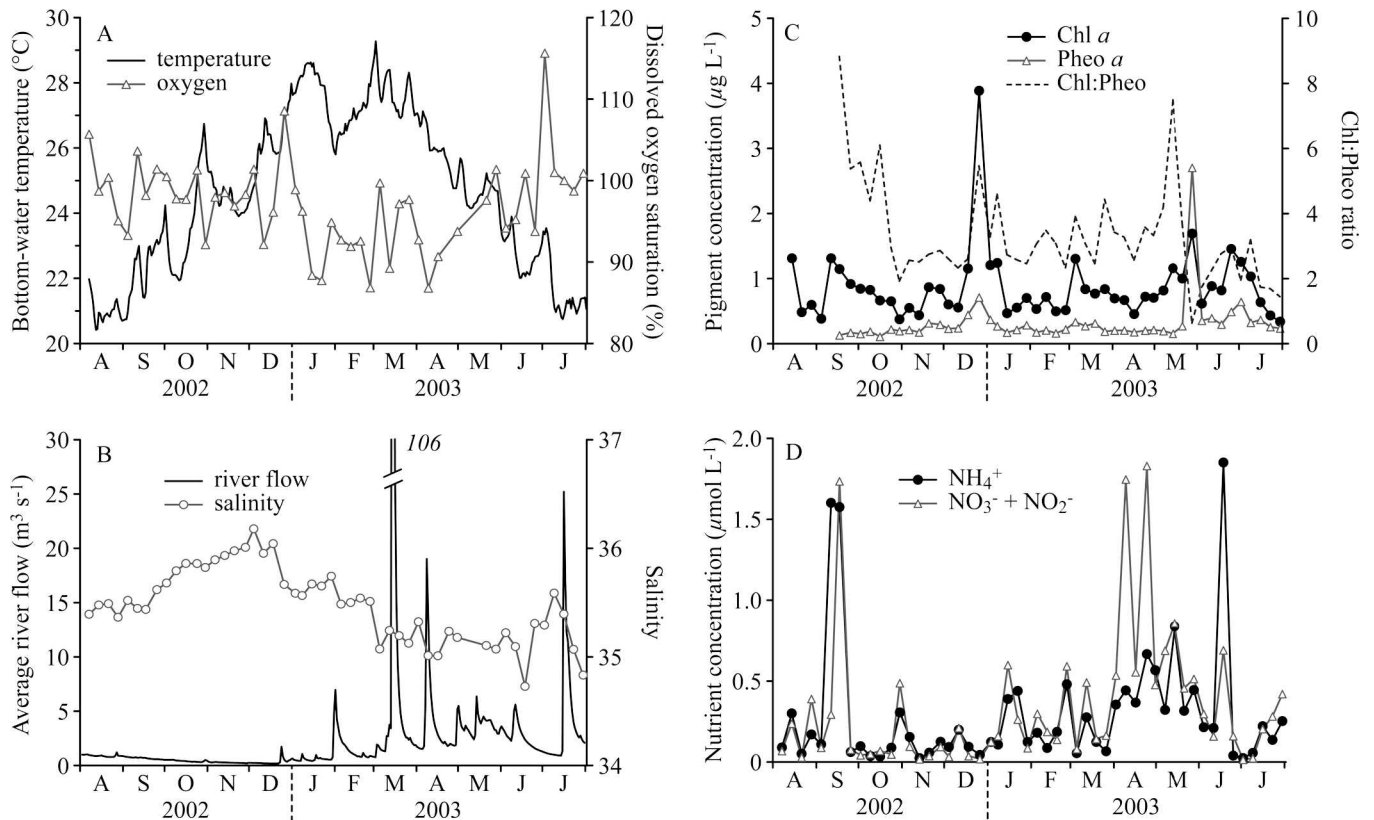


Fig. 5. Temporal variations of physical, chemical, and biological variables measured in bottom water from August 2002 to July 2003. (A) Temperature and dissolved oxygen saturation. (B) Salinity and Coulee River flow. (C) Chlorophyll *a* concentration, pheophytin *a* concentration, and Chl:Pheo mass ratio. (D) Ammonium and nitrate + nitrite concentrations.

Table 1. Pearson correlation coefficient matrix used to identify significant relationships between measured geochemical, physical, chemical, and biological variables.

		b	c	d	e	f	g	h	i	j
Average Ba : Ca	a	0.232**	0.111 <sup>ns</sup>	0.066 <sup>ns</sup>	0.319 <sup>ns</sup>	-0.027 <sup>ns</sup>	-0.002 <sup>ns</sup>	-0.122 <sup>ns</sup>	0.699**	0.155 <sup>ns</sup>
Average Mo : Ca	b		-0.322**	-0.411*	0.199 <sup>ns</sup>	0.080 <sup>ns</sup>	0.449*	0.424*	0.323 <sup>ns</sup>	0.349 <sup>ns</sup>
Temperature	c			0.108 <sup>ns</sup>	-0.423*	0.074 <sup>ns</sup>	-0.133 <sup>ns</sup>	0.064 <sup>ns</sup>	0.102 <sup>ns</sup>	-0.038 <sup>ns</sup>
Salinity	d				0.002 <sup>ns</sup>	-0.377*	-0.352*	-0.405*	-0.009 <sup>ns</sup>	-0.191 <sup>ns</sup>
DO saturation	e					-0.092 <sup>ns</sup>	-0.028 <sup>ns</sup>	-0.389*	0.504**	0.281 <sup>ns</sup>
Coulée River flow	f						0.070 <sup>ns</sup>	0.259 <sup>ns</sup>	-0.077 <sup>ns</sup>	0.046 <sup>ns</sup>
Ammonium	g							0.602**	0.032 <sup>ns</sup>	-0.011 <sup>ns</sup>
Nitrates + nitrites	h								-0.088 <sup>ns</sup>	-0.054 <sup>ns</sup>
Chlorophyll <i>a</i>	i									0.434*
Pheophytin <i>a</i>	j									

\*  $p < 0.01$ .

\*\*  $p < 0.001$ .

<sup>ns</sup>  $p > 0.01$ .

extent, in late December 2002 (Shell Nos. 1 and 3, no record in Shell No. 2) and March 2003 (all shells). The similarity of Mo:Ca time series of the three shells allowed us to build an average profile (Fig. 7B). Its background level was not constant but tended to present seasonal variations, with lowest values around the transition between the dry and wet seasons (December 2002). This seasonal pattern was almost in antiphase with the seasonal profiles of temperature and salinity. This is highlighted by the existence of significant negative correlations between

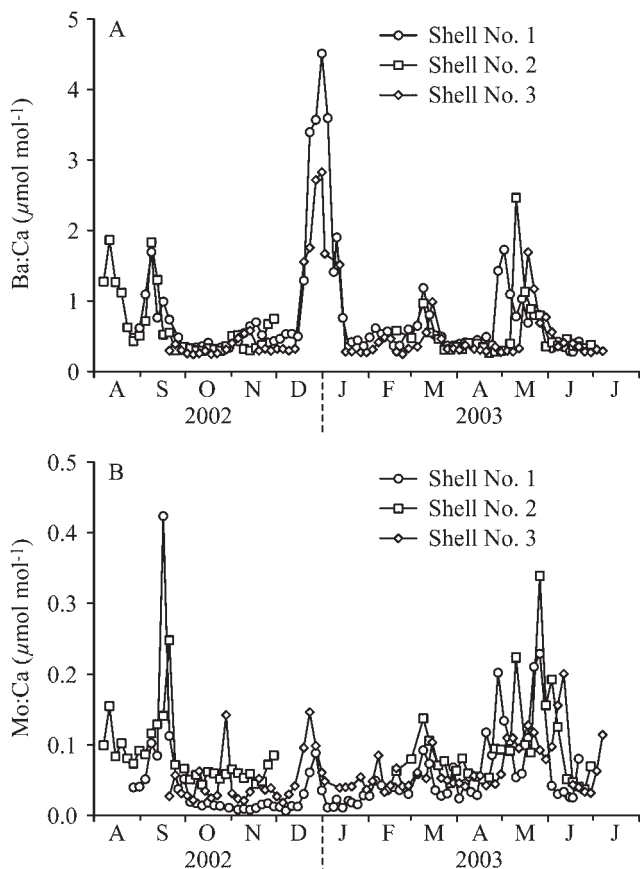


Fig. 6. Time series of elemental ratios archived in shells of three *C. radula* specimens. (A) Ba:Ca. (B) Mo:Ca.

Mo:Ca and these two variables (Table 1). Mo:Ca tended to be higher when the concentration of inorganic forms of nitrogen were elevated (Fig. 7B), an observation confirmed by significant correlations between Mo:Ca, and  $\text{NH}_4^+$  and  $\text{NO}_x^-$  concentrations ( $r^2 > 0.42$ ,  $p < 0.01$ ; Table 1).

Periods of high Mo:Ca were synchronous with high Ba:Ca in shells (Fig. 6). This is highlighted by a significant relationship between average profiles of Ba:Ca and Mo:Ca (Table 1). The weakness of this correlation, however, suggested that this relationship was not linear. This correlation was slightly higher according to the Spearman rank correlation coefficient ( $r = 0.455$ ,  $p < 0.001$ ), which indicated a certain synchronism of Ba:Ca and Mo:Ca peaks in shells.

Temporal variations of daily Ba and Mo incorporation rates were similar for all three specimens (Fig. 7C,D). The shape of these profiles was similar to the shape of Ba:Ca and Mo:Ca time series (i.e., a background level punctuated by sharp episodic peaks). Background levels, however, increased over the life of the scallops, reflecting the increase in the shell precipitation rate (Fig. 3D). Ba incorporation rate varied from 3.0 to 560.0  $\text{ng d}^{-1}$ , with a maximum rate recorded in late December 2002 (Fig. 7C). Mo incorporation rate was one order of magnitude smaller, ranging from 0.2 to 43.2  $\text{ng d}^{-1}$  and reaching a maximum in late May 2003 (Fig. 7D).

## Discussion

**Barium**—The high intershell reproducibility of Ba:Ca profiles suggests that the occurrence of Ba:Ca peaks was controlled by an environmental factor. There are, however, some inconsistencies in the timing of Ba:Ca peaks between shells in May 2003 (2-week time lag between Ba:Ca peaks of Shell Nos. 1 and 3) and, to a lesser extent, in March 2003 (Ba:Ca peak in Shell No. 3 appeared 1 week after those in the two other shells). These discrepancies are likely due to the uncertainty in the timing of geochemical records. The characteristics of Ba:Ca profiles (flat background level punctuated by sharp peaks; Figs. 6A, 7A) are similar to those observed in other bivalve species (Stecher et al. 1996; Vander Putten et al. 2000; Gillikin et al. 2008). This suggests that the choice of the shell surface or the outer shell layer for geochemical analyses has no significant

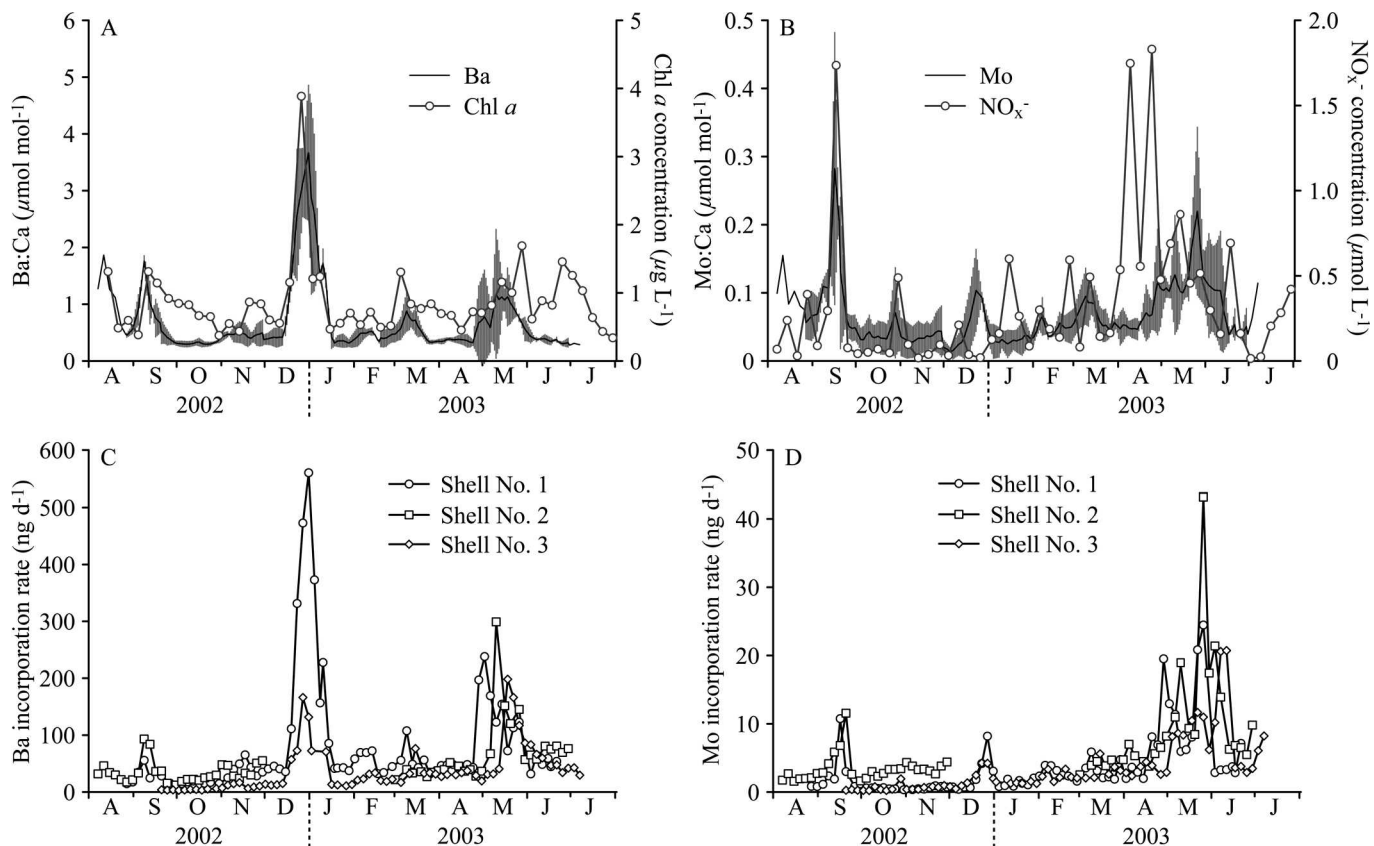


Fig. 7. (A, B) Average profiles of elemental ratios in *C. radula* shells ( $\pm 1\sigma$ ) overlain with environmental data. (A) Ba : Ca and Chl *a* concentration. (B) Mo : Ca and  $\text{NO}_x^-$  concentration. (C, D) Temporal variations of trace element incorporation rates in shells of three *C. radula* specimens. (C) Barium. (D) Molybdenum.

influence on Ba : Ca records in shells. In this section, we discuss the merits of several plausible hypotheses to explain temporal variability of Ba : Ca in *C. radula*.

Ba geochemistry in coastal environments is strongly controlled by fluvial inputs (Coffey et al. 1997). Although coastal cycling of Ba is quite complex, a general common pattern is a release of dissolved Ba from riverborne suspended matter during estuarine mixing, followed by conservative mixing with oceanic water. The magnitude of dissolved Ba release is dependent on the fluvial supply of suspended particulate matter. Gillikin et al. (2006) showed in both laboratory and field experiments that dissolved Ba concentration had an influence on the shell chemistry of *M. edulis*, controlling the background level of Ba : Ca. In our case, the main Ba : Ca peak occurred right after the dry season, when river flows were very low. Moreover, the highest flows were not synchronous with important Ba : Ca peaks, and no correlation was observed between Ba : Ca, river flow and salinity (Table 1). Therefore, variations in fluvial Ba inputs cannot explain Ba : Ca peaks in *C. radula*. A fluvial influence on Ba : Ca background level cannot be completely excluded. However, the absence of dissolved Ba concentration measurements in seawater keeps us from being assertive.

The high similarity of Chl *a* concentration and Ba : Ca time series and the close timing of Chl *a* and Ba : Ca peaks

strongly suggest a linkage between phytoplankton biomass and Ba incorporation into *C. radula* shells (Fig. 7A). Considering the uncertainty in time registration, we cannot conclude the exact duration of the time offset between Chl *a* and Ba : Ca peaks. The most that can be said is that, in general, Ba : Ca peaks tend to occur about a week after a Chl *a* peak. The ingestion of  $\text{BaSO}_4$  crystals formed after a phytoplankton bloom has been advanced as a possible explanation for Ba : Ca peaks observed in several other bivalve species (e.g., Stecher et al. 1996; Gillikin et al. 2006). According to Stecher and Kogut (1999), marine barite precipitation likely involves the biologic uptake of dissolved Ba by phytoplankton (or the abiotic adsorption of Ba on phytoplankton cell surfaces, e.g., onto iron oxyhydroxides; Sternberg et al. 2005), resulting in high amounts of Ba-rich particles. This first step is followed by a release of dissolved Ba and by an increase in  $\text{SO}_4^{2-}$  concentration during phytoplankton cell lysis, leading to the formation of  $\text{BaSO}_4$  crystals. This mechanism was advanced to explain the rapid and nearly complete removal of dissolved Ba in the Delaware estuary at the end of the 1996 spring bloom (Stecher and Kogut 1999).

The best conditions for barite formation are found within microenvironments originating from assemblages of recently dead diatoms (Bishop 1988). A long-term hydrological survey conducted from November 1999 to January

2003 showed that diatoms represented >90% of the total microalgal abundance in Sainte-Marie Bay (Jacquet et al. 2006). The weight of evidence indicates that most Chl *a* peaks observed during our survey likely reflected diatom blooms, an argument in support of the diatom-associated barite hypothesis. The absence of Ba:Ca peaks in shells at the end of May and June 2003 could mean that phytoplankton blooms recorded on 28 May 2003 and 25 June 2003 were dominated by other phytoplankton classes (e.g., dinophytes or coccolithophorids; Jacquet et al. 2006). This being so, could the amount of barite eventually precipitated within settling diatom flocs explain the quantity of Ba found in *C. radula* shells? Ba concentration has been measured in different marine diatom species cultured in artificial media, in natural seawater, or collected at sea (Riley and Roth 1971; Dehairs et al. 1980; Fisher et al. 1991). It ranges from 3 to 248  $\mu\text{g g}^{-1}$  of dry phytoplankton weight (average = 63  $\mu\text{g g}^{-1}$ ). On the basis of this average value and given our estimate of dry phytoplankton biomass during our survey (34–389  $\mu\text{g L}^{-1}$ ), the amount of Ba adsorbed onto diatom cells would have ranged from 2 to 25  $\text{ng L}^{-1}$ . According to Ganeshram et al. (2003), <4% of this Ba pool is converted to barite. This means that the amount of Ba that could be ingested by *C. radula* as barite crystals ranged, at most, between 0.08 and 1  $\text{ng L}^{-1}$ . In comparison, the daily rate of Ba incorporation into shells was 3–560  $\text{ng d}^{-1}$  (Fig. 7C). No data are available on filtration and ingestion rates of *C. radula*. Nevertheless, scallops are known to be able to filter  $\sim 5 \text{ L h}^{-1} \text{ g}^{-1}$  dry weight of soft parts at optimum temperature conditions (Palmer 1980; Laing 2004). Given the relationship between dry weight (*W*, g) of soft parts and shell height (*H*, mm) derived from the biological survey conducted by Thébault (2005) on *C. radula* ( $W = 3.89 \times 10^{-6} \times H^{3.066}$ ;  $r^2 = 0.827$ ,  $n = 441$ ), we estimated that specimens with shell height ranging from 20 to 60 mm filter between 5 and 132 liters of seawater daily. Although our calculations are only approximations, they show that the ingestion of the whole pool of barite originating from the decay of diatom blooms can only explain a small part of the amount of Ba incorporated daily within the shell.

Diatoms might be involved in the formation of Ba:Ca peaks through another process. Sternberg et al. (2005) demonstrated that high amounts of Ba can be adsorbed on iron oxyhydroxides associated with diatom frustules. Indeed, high iron (Fe) concentrations in the external medium unavoidably result in precipitation of iron oxyhydroxides onto cell surfaces (Morel and Hering 1993). The intensity of this process strongly increases when pH rises above 8 (see fig. 4 in Sternberg et al. 2005). Weathering of New Caledonian soils, largely composed of ultrabasic rocks (peridotites), into laterites enriched in transition metals induces important Fe inputs in the lagoon (Ambatsian et al. 1997). Because seawater pH ranged between 8.1 and 8.3 on our study site (Thébault 2005), high amounts of dissolved Ba could have been adsorbed onto iron oxyhydroxides precipitated onto diatom frustules during blooms. After ingestion of such Ba-rich diatoms by *C. radula*, a portion of Ba associated with iron oxyhydroxides could possibly be desorbed because of the

action of low gut pH and absorbed across the gut epithelium to reach the internal fluids before being sequestered into the shell. Considering our estimates (1) of the amount of Ba adsorbed onto diatom cells (2–25  $\text{ng L}^{-1}$ ; see previous paragraph), (2) of the daily rate of Ba incorporation in shells (3–560  $\text{ng d}^{-1}$ ; Fig. 7C), and (3) of *C. radula* filtration capacities (5–132  $\text{L d}^{-1}$ ; see previous paragraph), we conclude that the ingestion of the Ba pool adsorbed on diatom frustules (or at least a fraction of this pool) could explain the amount of Ba incorporated daily within the shell. The same line of reasoning might also apply to microphytobenthos. In the absence of benthic Chl *a* concentration measurements, no clear conclusion can be drawn about the possible influence of these microalgae on shell chemistry, although we know microphytobenthic production is high and dominated by diatoms in the southwest lagoon of New Caledonia (Clavier and Garrigue 1999; Clavier et al. 2005). Resuspension of benthic diatoms by *C. radula*'s valve movements and their subsequent ingestion might have induced high Ba:Ca in shells during periods of high benthic primary production.

**Molybdenum**—Profiles of Mo:Ca in *C. radula* have a similar shape (episodic increases over a background level) to those obtained in *P. maximus* from western France (Barats et al. 2007), suggesting ubiquitous Mo signals in scallop shells. The synchronism of Ba:Ca and Mo:Ca peaks suggests that the process or processes responsible for their temporal variations might share, to some extent, a common origin. An environmental control of Mo:Ca is likely, given the good intershell reproducibility. Several hypotheses, discussed in the next paragraphs, address the formation of Mo:Ca peaks.

Given the significant negative correlation observed between Mo:Ca and salinity (Table 1), Mo:Ca variations in *C. radula* shells could partly result from variations in freshwater inputs. However, a careful examination of Mo:Ca and salinity time series (Figs. 5B, 6B) reveals that freshwater input variations might explain the seasonal variations of Mo:Ca background level but not Mo:Ca peaks. Mo concentration is  $\sim 20$  times lower in rivers than in seawater (Morford and Emerson 1999). Therefore, it is unlikely that river inputs could have had a significant effect on Mo concentration in seawater and further in shells. On the other hand, freshwater inputs coming from minimally treated sewage of Nouméa could present significant levels of dissolved Mo, this metal being widely used in industry (e.g., in alloys). An influence of wastewater inputs on Mo:Ca background level cannot be excluded. This conclusion must be considered with care, however, in that this background level was sometimes below the limit of quantification of the LA-ICP-MS method.

High Mo concentrations are found in reducing sediments, primarily in association with manganese oxides ( $\text{MnO}_x$ ; Chaillou et al. 2002). Remobilization of this Mo pool during  $\text{MnO}_x$  reduction induces a release of dissolved Mo in pore water, leading to high concentrations in overlying waters (Chaillou et al. 2002). This upward transport of Mo is controlled by bioturbation and the Mo concentration gradient between pore and bottom

waters (Dalai et al. 2005). Enhanced supply of organic matter because of high productivity results in faster redox changes in sediments, yielding a steeper Mo concentration gradient and sudden increases in dissolved Mo concentration in bottom water (Dalai et al. 2005). Such a mechanism might have induced higher Mo concentration in internal fluids and finally in shells, explaining Mo:Ca peaks. There is little to support this assumption. The maximal phytoplankton biomass, which could have led to suboxic conditions at the sediment–water interface (see Fig. 5A for the sharp drop in DO saturation at the end of December 2002), was not synchronous with major Mo:Ca peaks. Moreover, Mo release out of the sediment occurs as molybdate ions ( $\text{MoO}_4^{2-}$ ), the soluble form of Mo in seawater (Chaillou et al. 2002). Metal bioaccumulation in marine organisms, although influenced by multiple routes of exposure (particles entering through the digestive gland and dissolved elements entering through the gills), is strongly influenced by the dietary uptake of metal bound to particles, especially in bivalves (Luoma and Rainbow 2005). Bustamante and Miramand (2005) found that most of the Mo contained in soft parts of the scallop *Chlamys varia* was located in the digestive gland (42–56% of total Mo compared with 5–8% in the gills). Nørum et al. (2005) also found that the Mo content in the digestive gland of the spiny and Pacific scallops was one order of magnitude higher than in the gills. Most of the Mo sequestered into scallop shells then could have a dietary origin. Hence, it seems unlikely that Mo:Ca peaks would originate from the efflux of dissolved Mo out of the sediment.

Another hypothesis is a linkage between Mo:Ca and phytoplankton dynamics. Mo usually behaves conservatively in seawater (Collier 1985). However, Dellwig et al. (2007) observed a nonconservative behavior of dissolved Mo in the Wadden Sea in relationship with algae blooms and bacterial activity; a phytoplankton bloom breakdown resulted in the release of high amounts of organic compounds by cell lyses, accelerating bacterial activity and promoting the formation of large aggregates. Bacterial activity in these aggregates induced the creation of suboxic microzones, which enabled fixation of Mo (Dellwig et al. 2007). Sedimentation and subsequent ingestion of such Mo-enriched aggregates might provide an explanation for Mo:Ca peaks observed in *C. radula*. However, significant correlations were observed in Sainte-Marie Bay between Chl *a* concentration and primary production and between primary production and bacterial production (S. Jacquet unpubl.). Mo-enriched aggregate sedimentation, and subsequent Mo incorporation into the shell, would then have reached a maximum in December 2002, which was not the case. Moreover, weekly SCUBA (self contained underwater breathing apparatus) diving on the study site revealed the absence of large aggregates in the water column. On the basis of these arguments, a relationship between Mo:Ca peaks and sedimentation of Mo-enriched aggregates originating from algal decay can hardly be deduced.

Mo is an essential cofactor of two enzymes responsible for nitrogen reduction in marine organisms: nitrate reductase and nitrogenase (Collier 1985), the latter being

exclusively found in  $\text{N}_2$ -fixing prokaryotes (primarily cyanobacteria). Many  $\text{N}_2$ -fixing cyanobacteria have been reported, but *Trichodesmium* spp. and *Richelia intracellularis* are traditionally considered the dominant marine diazotrophs (Sellner 1997). We did not observe *Trichodesmium* blooms on our study site during our survey. Although found in several bays around Nouméa, *R. intracellularis* was not reported in Sainte-Marie Bay (Jacquet et al. 2006). Moreover,  $\text{N}_2$  fixation is greatly decreased, or even completely inhibited, when alternative sources of inorganic nitrogen are available (Cheng et al. 1999). These alternative N sources were never depleted during our survey (range  $[\text{NH}_4^+ + \text{NO}_3^- + \text{NO}_2^-] = 0.04\text{--}3.31 \mu\text{mol L}^{-1}$ ). If Mo:Ca peaks had been formed after the ingestion of  $\text{N}_2$ -fixing cyanobacteria, these peaks would have occurred during periods when dissolved inorganic nitrogen concentration was low. Yet we observed a positive correlation between Mo:Ca ratio and nitrogenous nutrient concentrations (Table 1). Hence, it is quite unlikely that Mo:Ca peaks would have been formed after the ingestion of  $\text{N}_2$ -fixing cyanobacteria by *C. radula*.

A more plausible hypothesis might be a linkage between Mo:Ca in shells and the activity of nitrate reductase (NR). Phytoplankton need a source of nitrogen for the synthesis of organic compounds.  $\text{NH}_4^+$  is the primary inorganic nitrogen form entering the biosynthetic pathways.  $\text{NO}_3^-$  is also used but first needs to be reduced into  $\text{NO}_2^-$  by means of the assimilatory NR. The synthesis of this enzyme is induced by the presence of  $\text{NO}_3^-$  and coupled with an active uptake of Mo from seawater (Marino et al. 2003). This implies variable NR activity and Mo concentration in phytoplankton cells, depending on the nitrogen source used for biosynthesis. Because Mo:Ca was significantly correlated to  $\text{NO}_3^-$  concentration (Table 1), Mo incorporation into *C. radula* shell could come from the ingestion of phytoplankton cells grown on  $\text{NO}_3^-$ , therefore containing high intracellular levels of Mo for NR activity. However, maximum Mo:Ca was not recorded simultaneously with the maximum algal biomass (December 2002). Actually, this phytoplankton bloom probably grew primarily on  $\text{NH}_4^+$ . Very low  $\text{NH}_4^+$  concentrations can be sufficient to satisfy the nitrogen demand of phytoplankton because this compound can be regenerated rapidly by the heterotrophs in the water column. Indeed, Furnas et al. (2005) showed that  $\text{NH}_4^+$  pools in the Great Barrier Reef Lagoon can turn over within  $\leq 1$  d. This is shorter than  $\text{NO}_3^-$  turnover time and than the frequency of our hydrological survey (1 week). Few data are available concerning Mo requirements for phytoplankton growth. Raven (1988) estimated that photolithotrophs growing on  $\text{NO}_3^-$  need  $9.63 \mu\text{g Mo g}^{-1}$  dry weight for a relative growth rate of  $3 \times 10^{-5} \text{ s}^{-1}$  at  $20^\circ\text{C}$  (with C = 50% of dry weight). According to this value, our estimate of dry phytoplankton biomass during our survey ( $34\text{--}389 \mu\text{g L}^{-1}$ ) corresponded to a Mo pool of  $0.3\text{--}3.7 \text{ ng L}^{-1}$ . In our study, the daily rate of Mo incorporation in shells was  $0.2\text{--}43.2 \text{ ng d}^{-1}$  (Fig. 7D). Given our estimate of *C. radula* filtration capacities, the intracellular pool of Mo carried by phytoplankton growing on  $\text{NO}_3^-$  could explain the amount of Mo incorporated daily within the shell. A relationship might also exist

between the formation of Mo:Ca peaks in shells and the ingestion of important amounts of resuspended microphytobenthos cells grown on  $\text{NO}_3^-$ .

In this paper, we presented intriguing and definitely promising records of Ba:Ca and Mo:Ca ratios in bivalve mollusk shells. Although this study relied on only three specimens, the high interindividual reproducibility of Ba:Ca and Mo:Ca profiles suggests that incorporation of these elements within the shells was controlled by environmental forcings. Fluvial Ba inputs in the lagoon do not provide a satisfactory explanation for Ba:Ca peak formation in *C. radula* shells. Given the lack of a strong argument for or against this hypothesis, we cannot exclude that the ingestion of diatom-associated barite crystals is involved in the formation of Ba:Ca peaks. Our study should definitely be repeated with measurements of barite concentration in seawater and in the digestive tract of *C. radula* to conclude that the ingestion of barite crystals can (or cannot) explain, at least partly, the formation of Ba:Ca peaks. On the other hand, our results, coupled with those of Sternberg et al. (2005), suggest that the ingestion of diatom cells enriched in Ba (adsorbed on iron oxyhydroxides associated with the frustules) is the most plausible hypothesis. If this reasoning is correct, the Ba:Ca ratio would be a proxy for the timing and magnitude of diatom blooms. Several hypotheses were discussed to explain the formation of Mo:Ca peaks: (1) freshwater Mo inputs in the lagoon, (2) the release of Mo out of the sediment during the development of anoxic conditions at the sediment–water interface, (3) the ingestion of Mo-enriched aggregates originating from algal decay, (4) the ingestion of  $\text{N}_2$ -fixing cyanobacteria, and (5) the ingestion of phytoplankton cells grown on  $\text{NO}_3^-$  and containing high levels of Mo for the activity of nitrate reductase. Although wastewater inputs coming from Nouméa might have an influence on the Mo:Ca background level, Mo:Ca peaks would be more likely to come from the ingestion of phytoplankton cells containing nitrate reductase. Mo:Ca could then be a proxy for  $\text{NO}_3^-$  uptake by phytoplankton in coastal ecosystems, which would contribute to our understanding of the historical balance between new and regenerated production. Further work, such as experiments under semi-controlled conditions (feeding studies within benthic chambers), is necessary to confirm these two elements as proxies. We conclude with confirmation that Ba:Ca is an interesting tool, albeit still poorly understood, for describing historical phytoplankton dynamics, and the introduction of Mo:Ca is a promising addition to the arsenal of proxies.

#### Acknowledgments

We are grateful to Tara Schraga (U.S. Geological Survey [USGS], Menlo Park, California) for linguistic corrections to this manuscript. We also thank Sandrine Chifflet, Philippe Gérard, Alain Lapetite, and Christophe Peignon (Institut de Recherche pour le Développement [IRD], Nouméa, New Caledonia) for laboratory and field assistance. Special thanks are due to James E. Cloern (USGS) and Bernd R. Schöne (University of Mainz, Germany) for their constructive comments on an earlier version of the manuscript. Thermo Electron Company is thanked for loan of the X7 series inductively coupled plasma mass spectrometer (ICP-

MS). This manuscript has greatly benefited from critical reviews and very helpful comments by David P. Gillikin and Jody Stecher.

This study was supported by the IRD, the Région Bretagne, the French Programme National Environnement Côtier, and the French Ministry of Research's Actions Concertées Incitatives—Jeunes Chercheurs program (ACI-PECTEN).

#### References

- AMBATSIAN, P., F. FERNEX, M. BERNAT, C. PARRON, AND J. LECOLLE. 1997. High metal inputs to closed seas: The New Caledonian lagoon. *J. Geochem. Explor.* **59**: 59–74.
- AVERYT, K. B., AND A. PAYTAN. 2004. A comparison of multiple proxies for export production in the equatorial Pacific. *Paleoceanography* **19**: PA4003, doi:10.1029/2004PA001005.
- BARATS, A., C. PÉCHEYRAN, D. AMOUROUX, S. DUBASCOUX, L. CHAUVAUD, AND O. F. X. DONARD. 2007. Matrix-matched quantitative trace element analysis in calcium carbonate shells by laser ablation ICP-MS: Application to the determination of daily scale profiles in scallop shell (*Pecten maximus*). *Anal. Bioanal. Chem.* **387**: 1131–1140.
- BENSON, B. B., AND D. KRAUSE. 1984. The concentration and isotopic fractionation of oxygen dissolved in freshwater and seawater in equilibrium with the atmosphere. *Limnol. Oceanogr.* **29**: 620–632.
- BISHOP, J. K. B. 1988. The barite–opal–organic carbon association in oceanic particulate matter. *Nature* **332**: 341–343.
- BUJAN, S. 2000. Biogeochemical modelling of carbon and nitrogen cycles in tropical ecosystems under terrigenous and anthropogenic influences—a case study in the lagoon of Nouméa (New Caledonia). Ph.D. thesis. Univ. Méditerranée. [In French.]
- BUSTAMANTE, P., AND P. MIRAMAND. 2005. Subcellular and body distributions of 17 trace elements in the variegated scallop *Chlamys varia* from the French coast of the Bay of Biscay. *Sci. Total Environ.* **337**: 59–73.
- CARPENTER, J. H. 1965. The accuracy of the Winkler method for dissolved oxygen analysis. *Limnol. Oceanogr.* **10**: 135–140.
- CARRÉ, M., I. BENTALEB, O. BRUGUIER, E. ORDINOLA, N. T. BARRETT, AND M. FONTUGNE. 2006. Calcification rate influence on trace element concentrations in aragonitic bivalve shells: Evidences and mechanisms. *Geochim. Cosmochim. Acta* **70**: 4906–4920.
- CHAILLOU, G., P. ANSCHUTZ, G. LAVAUX, J. SCHAFER, AND G. BLANC. 2002. The distribution of Mo, U, and Cd in relation to major redox species in muddy sediments of the Bay of Biscay. *Mar. Chem.* **80**: 41–59.
- CHARPY, L., AND C. J. CHARPY-ROUBAUD. 1990. Trophic structure and productivity of the lagoonal communities of Tikehau atoll (Tuamotu Archipelago, French Polynesia). *Hydrobiologia* **207**: 43–52.
- CHAUVAUD, L., G. THOUZEAU, AND Y.-M. PAULET. 1998. Effects of environmental factors on the daily growth rate of *Pecten maximus* juveniles in the Bay of Brest (France). *J. Exp. Mar. Biol. Ecol.* **227**: 83–111.
- CHENG, J., C. R. HIPKIN, AND J. R. GALLON. 1999. Effects of inorganic nitrogen compounds on the activity and synthesis of nitrogenase in *Gloeotheca* (Nägeli) sp. ATCC 27152. *New Phytol.* **141**: 61–70.
- CLAVIER, J., AND C. GARRIGUE. 1999. Annual sediment primary production and respiration in a large coral reef lagoon (SW New Caledonia). *Mar. Ecol. Prog. Ser.* **191**: 79–89.
- , G. BOUCHER, L. CHAUVAUD, R. FICHEZ, AND S. CHIFFLET. 2005. Benthic response to ammonium pulses in a tropical lagoon: Implications for coastal environmental processes. *J. Exp. Mar. Biol. Ecol.* **316**: 231–241.

- COFFEY, M., F. DEHAIRS, O. COLLETTE, G. LUTHER, T. CHURCH, AND T. JICKELLS. 1997. The behaviour of dissolved barium in estuaries. *Estuar. Coast. Shelf Sci.* **45**: 113–121.
- COLLIER, R. W. 1985. Molybdenum in the northeast Pacific Ocean. *Limnol. Oceanogr.* **30**: 1351–1354.
- CURRIE, L. A. 1995. Nomenclature in evaluation of analytical methods including detection and quantification capabilities. *Pure Appl. Chem.* **67**: 1699–1723.
- DALAI, T. K., K. NISHIMURA, AND Y. NOZAKI. 2005. Geochemistry of molybdenum in the Chao Phraya River estuary, Thailand: Role of suboxic diagenesis and porewater transport. *Chem. Geol.* **218**: 189–202.
- DEHAIRS, F., R. CHESSELET, AND J. JEDWAB. 1980. Discrete suspended particles of barite and the barium cycle in the open ocean. *Earth Planet. Sci. Lett.* **49**: 528–550.
- DELLWIG, O., M. BECK, A. LEMKE, M. LUNAU, K. KOLDITZ, B. SCHNETGER, AND H.-J. BRUMSACK. 2007. Non-conservative behaviour of molybdenum in coastal waters: Coupling geochemical, biological, and sedimentological processes. *Geochim. Cosmochim. Acta* **71**: 2745–2761.
- FIELD, C. B., M. J. BEHRENFELD, J. T. RANDERSON, AND P. FALKOWSKI. 1998. Primary production of the biosphere: Integrating terrestrial and oceanic components. *Science* **281**: 237–240.
- FISHER, N. S., R. R. L. GUILLARD, AND D. C. BANKSTON. 1991. The accumulation of barium by marine phytoplankton grown in culture. *J. Mar. Res.* **49**: 339–354.
- FURNAS, M., A. MITCHELL, M. SKUZA, AND J. BRODIE. 2005. In the other 90%: Phytoplankton responses to enhanced nutrient availability in the Great Barrier Reef Lagoon. *Mar. Pollut. Bull.* **51**: 253–265.
- GANESHAM, R. S., R. FRANÇOIS, J. COMMEAU, AND S. L. BROWN-LEGER. 2003. An experimental investigation of barite formation in seawater. *Geochim. Cosmochim. Acta* **67**: 2599–2605.
- GILLKIN, D. P., F. DEHAIRS, A. LORRAIN, D. STEENMANS, W. BAEYENS, AND L. ANDRÉ. 2006. Barium uptake into the shells of the common mussel (*Mytilus edulis*) and the potential for estuarine paleo-chemistry reconstruction. *Geochim. Cosmochim. Acta* **70**: 395–407.
- , A. LORRAIN, Y.-M. PAULET, L. ANDRÉ, AND F. DEHAIRS. 2008. Synchronous barium peaks in high-resolution profiles of calcite and aragonite marine bivalve shells. *Geo-Mar. Lett.* **28**: 351–358.
- GRAY, A. L. 1985. Solid sample introduction by laser ablation for inductively coupled plasma source mass spectrometry. *The Analyst* **110**: 551–556.
- HENDERSON, G. M. 2002. New oceanic proxies for paleoclimate. *Earth Planet. Sci. Lett.* **203**: 1–13.
- HOLMES, M. R., A. AMINOT, R. KÉROUEL, B. A. HOOKER, AND B. J. PETERSON. 1999. A simple and precise method for measuring ammonium in marine and freshwater ecosystems. *Can. J. Fish. Aquat. Sci.* **56**: 1801–1808.
- ITTEKKOT, V., AND OTHERS. 1996. Oceans, p. 267–288. *In* R. T. Watson, M. C. Zinyowera and R. H. Moss [eds.], *Climate change 1995: Impacts, adaptations, and mitigation of climate change*. Cambridge Univ. Press.
- JACQUET, S., B. DELESALLE, J.-P. TORRÉTON, AND J. BLANCHOT. 2006. Response of phytoplankton communities to increased anthropogenic influences (southwestern lagoon, New Caledonia). *Mar. Ecol. Prog. Ser.* **320**: 65–78.
- LAING, I. 2004. Filtration of king scallops (*Pecten maximus*). *Aquaculture* **240**: 369–384.
- LORRAIN, A., D. P. GILLKIN, Y.-M. PAULET, L. CHAUVAUD, J. NAVEZ, A. LE MERCIER, AND L. ANDRÉ. 2005. Strong kinetic effects on Sr/Ca ratios in the calcitic bivalve *Pecten maximus*. *Geology* **33**: 965–968.
- LUOMA, S. N., AND P. S. RAINBOW. 2005. Why is metal bioaccumulation so variable? Biodynamics as a unifying concept. *Environ. Sci. Technol.* **39**: 1921–1931.
- MARINO, R., R. W. HOWARTH, F. CHAN, J. J. COLE, AND G. E. LIKENS. 2003. Sulfate inhibition of molybdenum-dependent nitrogen fixation by planktonic cyanobacteria under seawater conditions: A non-reversible effect. *Hydrobiologia* **500**: 277–293.
- MARKICH, S. J., AND R. A. JEFFREE. 1994. Absorption of divalent trace metals as analogues of calcium by Australian freshwater bivalves: An explanation of how water hardness reduces metal toxicity. *Aquat. Toxicol.* **29**: 257–290.
- MILLER, A. J., A. J. GABRIC, J. R. MOISAN, F. CHAI, D. J. NEILSON, D. W. PIERCE, AND E. DI LORENZO. 2006. Global change and oceanic primary productivity: Effects of ocean-atmosphere-biological feedbacks, p. 29–65. *In* H. Kawahata and Y. Awaya [eds.], *Global climate change and response of the carbon cycle in the Equatorial Pacific and Indian Oceans and adjacent landmasses*. Elsevier.
- MOREL, F., AND J. HERING. 1993. Principles and applications of aquatic chemistry. Wiley.
- MORFORD, J. L., AND S. EMERSON. 1999. The geochemistry of redox sensitive trace metals in sediments. *Geochim. Cosmochim. Acta* **63**: 1735–1750.
- NØRUM, U., V. W.-M. LAI, AND W. R. CULLEN. 2005. Trace element distribution during the reproductive cycle of female and male spiny and Pacific scallops, with implications for biomonitoring. *Mar. Pollut. Bull.* **50**: 175–184.
- PALMER, R. E. 1980. Behavioral and rhythmic aspects of filtration in the Bay scallop, *Argopecten irradians concentricus* (Say), and the oyster, *Crassostrea virginica* (Gmelin). *J. Exp. Mar. Biol. Ecol.* **45**: 273–295.
- RAIMBAULT, P., G. SLAWYK, B. COSTE, AND J. FRY. 1990. Feasibility of using an automated colorimetric procedure for the determination of seawater nitrate in the 0 to 100 nM range: Examples from field and culture. *Mar. Biol.* **104**: 347–351.
- RAVEN, J. A. 1988. The iron and molybdenum use efficiencies of plant growth with different energy, carbon and nitrogen sources. *New Phytol.* **109**: 279–287.
- RILEY, J. P., AND I. ROTH. 1971. The distribution of trace elements in some species of phytoplankton grown in culture. *J. Mar. Biol. Assoc. UK* **51**: 63–72.
- SARMIENTO, J. L., AND OTHERS. 2004. Response of ocean ecosystems to climate warming. *Glob. Biogeochem. Cycles* **18**: GB3003, doi:10.1029/2003GB002134.
- SCHÖNE, B. R., M. PFEIFFER, T. POHLMANN, AND F. SIEGISMUND. 2005. A seasonally resolved bottom-water temperature record for the period AD 1866–2002 based on shells of *Arctica islandica* (Mollusca, North Sea). *Int. J. Climatol.* **25**: 947–962.
- SELLNER, K. G. 1997. Physiology, ecology, and toxic properties of marine cyanobacteria blooms. *Limnol. Oceanogr.* **42**: 1089–1104.
- STECHER, H. A., AND M. B. KOGUT. 1999. Rapid barium removal in the Delaware estuary. *Geochim. Cosmochim. Acta* **63**: 1003–1012.
- , D. E. KRANTZ, C. J. LORD, G. W. LUTHER, AND K. W. BOCK. 1996. Profiles of strontium and barium in *Mercenaria mercenaria* and *Spisula solidissima* shells. *Geochim. Cosmochim. Acta* **60**: 3445–3456.
- STERNBERG, E., D. TANG, T.-Y. HO, C. JEANDEL, AND F. M. M. MOREL. 2005. Barium uptake and adsorption in diatoms. *Geochim. Cosmochim. Acta* **69**: 2745–2752.
- STRICKLAND, J. 1960. Measuring the production of marine phytoplankton. The Queen's Printer.

- TAKESUE, R. K., C. R. BACON, AND J. K. THOMPSON. 2008. Influences of organic matter and calcification rate on trace elements in aragonitic estuarine bivalve shells. *Geochim. Cosmochim. Acta* **72**: 5431–5445.
- THÉBAULT, J. 2005. The shell of the scallop, *Comptopallium radula* (Bivalvia; Pectinidae), eulerian high-frequency archives of the variability of tropical coastal environments (Pacific Ocean). Ph.D. thesis. Univ. Bretagne Occidentale. [In French.]
- , L. CHAUVAUD, J. CLAVIER, R. FICHEZ, AND E. MORIZE. 2006. Evidence of a 2-day periodicity of striae formation in the tropical scallop *Comptopallium radula* using calcein marking. *Mar. Biol.* **149**: 257–267.
- , AND OTHERS. 2007. Reconstruction of seasonal temperature variability in the tropical Pacific Ocean from the shell of the scallop, *Comptopallium radula*. *Geochim. Cosmochim. Acta* **71**: 918–928.
- VANDER PUTTEN, E., F. DEHAIRS, E. KEPPENS, AND W. BAEYENS. 2000. High resolution distribution of trace elements in the calcite shell layer of modern *Mytilus edulis*: Environmental and biological controls. *Geochim. Cosmochim. Acta* **64**: 997–1011.
- YENTSCH, C. S., AND D. W. MENZEL. 1963. A method for the determination of phytoplankton chlorophyll and phaeophytin by fluorescence. *Deep-Sea Res.* **10**: 221–231.

*Associate editor: John Albert Raven*

*Received: 23 July 2008*

*Accepted: 08 February 2009*

*Amended: 08 February 2009*